

Article

Effect of Copolymer Properties on the Phase Behavior of Ibuprofen–PLA/PLGA Mixtures

Anton Iemtsev ¹, Martin Klajmon ¹, Fatima Hassouna ² and Michal Fulem ^{1,*}

¹ Department of Physical Chemistry, University of Chemistry and Technology, Prague, Technická 5, 166 28 Prague, Czech Republic

² Faculty of Chemical Engineering, University of Chemistry and Technology, Prague, Technická 5, 166 28 Prague, Czech Republic

* Correspondence: fulemm@vscht.cz

Abstract: Prediction of compatibility of the active pharmaceutical ingredient (API) with the polymeric carrier plays an essential role in designing drug delivery systems and estimating their long-term physical stability. A key element in deducing API–polymer compatibility is knowledge of a complete phase diagram, i.e., the solubility of crystalline API in polymer and mutual miscibility of API and polymer. In this work, the phase behavior of ibuprofen (IBU) with different grades of poly(D,L-lactide-co-glycolide) (PLGA) and polylactide (PLA), varying in composition of PLGA and molecular weight of PLGA and PLA, was investigated experimentally using calorimetry and computationally by the perturbed-chain statistical associating fluid theory (PC-SAFT) equation of state (EOS). The phase diagrams constructed based on a PC-SAFT EOS modeling optimized using the solubility data demonstrated low solubility at typical storage temperature (25 °C) and limited miscibility (i.e., presence of the amorphous–amorphous phase separation region) of IBU with all polymers studied. The ability of PC-SAFT EOS to capture the experimentally observed trends in the phase behavior of IBU–PLA/PLGA systems with respect to copolymer composition and molecular weight was thoroughly investigated and evaluated.

Keywords: biodegradable polymers; PLGA; PLA; amorphous solid dispersion; API–polymer compatibility; PC-SAFT; phase diagrams



Citation: Iemtsev, A.; Klajmon, M.; Hassouna, F.; Fulem, M. Effect of Copolymer Properties on the Phase Behavior of Ibuprofen–PLA/PLGA Mixtures. *Pharmaceutics* **2023**, *15*, 645. <https://doi.org/10.3390/pharmaceutics15020645>

Academic Editors: Ildikó Bácskay and János Borbély

Received: 20 January 2023

Revised: 8 February 2023

Accepted: 10 February 2023

Published: 14 February 2023



Copyright: © 2023 by the authors. Licensee MDPI, Basel, Switzerland. This article is an open access article distributed under the terms and conditions of the Creative Commons Attribution (CC BY) license (<https://creativecommons.org/licenses/by/4.0/>).

1. Introduction

The poor bioavailability of many active pharmaceutical ingredients (APIs) represents one of the major challenges to successful pharmaceutical development [1]. Several strategies to tackle this problem have been developed, including the formation of polymeric amorphous solid dispersions (ASDs) [2], which consist of amorphous API molecularly dispersed in the polymer matrix, and the preparation of polymeric micro- and nanoparticles [3]. The design of these drug formulations is still governed to a large extent by trial-and-error approaches. An influential parameter determining the successful polymeric drug formulations, their physical stability, and performance-related characteristics is the compatibility of API with the polymer. The compatibility between API and polymer, which at the molecular level reflects the strength of their intermolecular interactions compared to API–API and polymer–polymer cohesive interactions, affects the phase behavior of API–polymer mixtures, such as the size of the immiscibility region (i.e., liquid–liquid equilibria (LLE)) or the solubility of crystalline API in the polymeric matrix (solid–liquid equilibrium (SLE)). SLE determines the maximum concentration of amorphous API that can be thermodynamically stabilized against the recrystallization in the polymer matrix, while LLE identifies the conditions (temperature and concentration) at which liquid–liquid or amorphous phase separation (APS) can occur. Both the recrystallization of API and APS can lead to undesirable heterogeneities of ASD formulations. An initial step in the polymeric drug formulation development is the selection of a suitable polymeric excipient,

which must be biocompatible and offer the desired formulation properties such as optimal API loading and physical stability over time. The latter properties are directly related to the compatibility of drug formulation components. As the number of initially identified biocompatible polymers for a given API can be high, it is highly desirable to develop efficient computational tools that would be capable of estimating or ranking the polymer compatibility with a given API.

Among various polymeric carriers, aliphatic polyesters have received a growing interest in the development of efficient drug delivery systems due to their unique properties including biocompatibility, biodegradability, and low toxicity. Within the biodegradable polyesters, poly(D,L-lactide-co-glycolide) (PLGA) and polylactide (PLA) represent particular relevance in drug delivery [4]. They have been FDA-approved [5]. Their degradation rate by hydrolysis is controlled by regulating the polymer molecular weight, the composition of monomer units in the copolymer (e.g., lactide (LA) to glycolide (GA) ratio in PLGA), and the type of stereo-forms of lactide units (i.e., D- and L-lactide) [6]. PLGA and PLA have proven themselves as effective polymeric carriers in the development of amorphous solid dispersions (ASDs) [7,8] and micro- or nanoparticle-based drug products formulation [9–13].

In our previous work [14], in which the phase behavior of various model APIs with two PLGA copolymers possessing a similar molecular weight (about 10,000 g/mol) but different LA to GA ratios (50:50 and 75:25) was studied, it was shown that the perturbed-chain statistical associating fluid theory (PC-SAFT) equation of state (EOS) in connection with calorimetric measurements of SLE curve is capable of predicting a complete phase diagram including amorphous phase separation (APS), which was found to be in agreement with a long-term behavior of the prepared formulations. The systems of ibuprofen (IBU) with both PLGA polymers showed very limited miscibility, which was demonstrated experimentally by APS during calorimetric measurements and long-term physical stability studies. This system is therefore ideal for exploring the capability of modeling tools, such as the perturbed-chain statistical associating fluid theory (PC-SAFT) equation of state (EOS), to capture the effect of copolymer molecular weight and composition on the size of immiscibility region (i.e., LLE), which is in API–polymer systems demonstrated by amorphous phase separation (APS). We note that, in general, LLE predictions using thermodynamic models are fairly challenging. The situation becomes even more complicated in the case of asymmetric mixtures such as API–polymer mixtures. In this work, the effect of composition and molecular weight of a range of PLA/PLGA polymers on the phase behavior (both SLE and LLE) of IBU was thoroughly investigated experimentally by calorimetry and computationally using PC-SAFT EOS.

2. Materials and Methods

2.1. Materials

Racemic IBU was kindly donated by Zentiva Group (Prague, Czech Republic). Two PLA commercial grades (Purasorb PDL 02A and PDL 04A) and two PLGA commercial grades (PDLG 5004A and PDLG 7504A) consisting of 50:50 and 75:25 of LA:GA units were graciously provided by Corbion (Gorinchem, The Netherlands). All chemicals were used without further purification. The molecular structures of the used chemicals are depicted in Figure 1, and their selected physicochemical properties are summarized in Section 3.1.

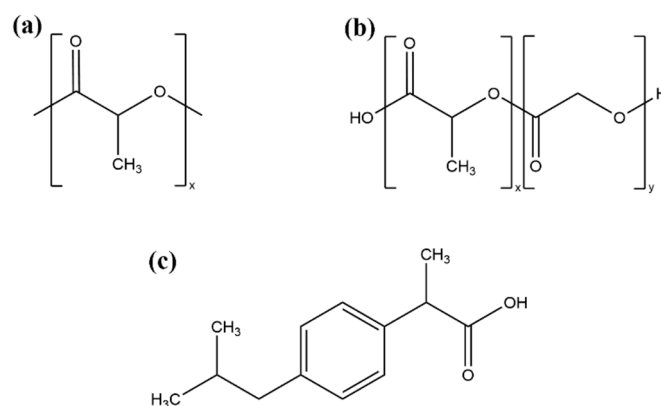


Figure 1. Chemical structures of used compounds: (a) PLA, (b) PLGA, and (c) IBU.

2.2. Experimental Methods

2.2.1. Differential Scanning Calorimetry

The differential scanning calorimetry (DSC) analysis was performed to determine the thermal properties of pure chemical compounds, measure SLE and glass transition temperatures (T_g), and map APS regions. TA Q1000 DSC from TA Instruments, Inc. (New Castle, DE, USA) calorimeter was used. All scans were carried out in the preselected temperature range (-90 to 150 °C) and nitrogen gas purge (50 mL min^{-1}).

The samples (5 – 10 mg) were placed in aluminum pans, which were tightly sealed and pinned in the lid to permit the evaporation of residual moisture that may be present in the polymer. A thorough calibration of temperature and enthalpy was performed using five reference materials: tin, indium, naphthalene, gallium, and water.

2.2.2. Calorimetric Determination of SLE Curve and Mapping of LLE Region

The solubility temperature (T_s) of IBU in PLA/PLGA polymers was experimentally determined using DSC. Several DSC protocols are described in the literature and generally applied for the measurement of the T_s : recrystallization (demixing) method [15], melting point depression (MPD) method [16], annealing method [17], melting enthalpy method [18], and step-wise dissolution method (S-WD) [19] (a DSC protocol recently developed in our research group). As the IBU–PLA/PLGA mixtures exhibited APS over a wide range of compositions, the S-WD protocol could not be applied in this work as it derives the solubility from the measured T_g of a homogenous amorphous system. The MPD method, the most frequently applied DSC protocol, was therefore selected and used in this study. The MPD procedure consists of measuring the melting temperature of API in the polymer matrix, which decreases with the increasing polymer concentration due to the reduction of API chemical potential in the API–polymer mixture.

The solubility temperatures T_s of IBU in PLA and PLGA polymers were determined from the melting endotherms of corresponding physical mixtures using the melting peak top (following Höhne et al. [20] recommendation), while the melting temperature (T_m) of the pure IBU was taken as the onset temperature of the melting peak. The physical mixtures were obtained by mild mixing of IBU with PLA/PLGA polymers in predetermined ratios for about 10 min using a pestle and mortar. T_s of IBU in the PLGA and PLA polymers were measured at the heating rate (β) of 1 °C min^{-1} (according to Höhne et al. [20] advising the application of β lower than 2 °C min^{-1}) during the first heating ramp, which was followed by the cooling ($\beta = 20$ °C min^{-1}) of the melt and second heating ramp ($\beta = 10$ °C min^{-1}) for the T_g determination. To map the immiscibility regions, i.e., the temperature-composition regions where APS occurs, IBU–PLGA and IBU–PLA mixtures with compositions ranging from 10 to 70 wt.% IBU were subject to successive heating–cooling–heating cycles during which T_g values of the system were measured. The upper temperature of the initial heating cycle was set slightly above T_m of IBU to 80 °C. Upper heating temperatures were subsequently increased by 10 °C in each successive cycle up to reaching the final

temperature of 150 °C. By this procedure, the temperature-concentration region from 10 to 70 wt.% IBU and from 80 °C to 150 °C was screened for each binary system for APS. If only a single T_g value was obtained during T_g determination, positioned between the value for pure amorphous IBU and polymer, the system was considered to consist of a single homogenous amorphous phase. If two T_g values were detected, the system was considered separated into two amorphous phases—IBU-rich and polymer-rich amorphous phases.

2.3. Modeling Approaches

2.3.1. Modeling of Glass-Transition Temperature

The Kwei equation [21] was used to model T_g lines for IBU-PLA/PLGA mixtures:

$$T_g = \frac{w_1 T_{g1} + k w_2 T_{g2}}{w_1 + k w_2} + q w_1 w_2 \quad (1)$$

where T_{g1} and T_{g2} are the glass-transition temperatures of the pure components, w_1 and w_2 are the mass fractions of each component, and k and q are parameters that can be obtained by fitting the experimental T_g values for a given binary mixture.

The Kwei equation (Equation (1)) can also be used with the parameter k estimated using the Simha-Boyer rule [22], which requires knowledge of T_g and density values for both pure components, followed by determination of the parameter q by fitting it to experimental binary T_g data. Since this approach leads to higher deviations from experimental T_g data [23], a simultaneous fitting of both parameters k and q to experimental T_g data was used to model T_g lines in this work.

2.3.2. SLE and LLE Modeling Using PC-SAFT EOS

Assuming that the crystalline phase consists of only pure IBU, the solubility of IBU in PLA/PLGA polymers x_{IBU}^L (IBU mole fraction in the liquid/amorphous phase) can be calculated using the following rigorous thermodynamic relationship:

$$x_{IBU}^L = \frac{1}{\gamma_{IBU}^L} \exp \left[-\frac{\Delta_{fus}H}{RT} \left(1 - \frac{T}{T_m} \right) - \frac{1}{RT} \int_{T_m}^T \Delta_{fus}C_p dT + \frac{1}{R} \int_{T_m}^T \frac{\Delta_{fus}C_p}{T} dT \right] \quad (2)$$

where T is the absolute temperature; T_m and $\Delta_{fus}H$ are the melting temperature and fusion enthalpy, respectively, of pure crystalline IBU; $\Delta_{fus}C_p$ is the difference between the isobaric molar heat capacity of the liquid and crystalline phases of IBU; R is the universal gas constant; and γ_{IBU}^L is the activity coefficient of IBU in the liquid IBU-polymer phase. As can be seen from Equation (2), SLE calculations require two types of thermodynamic data as the input: (i) thermodynamic fusion data for pure IBU (T_m , $\Delta_{fus}H$, and $\Delta_{fus}C_p$) and (ii) the activity coefficient γ_{IBU}^L reflecting the intermolecular interaction between the solute (IBU) and solvent (PLA/PLGA polymers). The fusion thermodynamic properties of pure solute are typically obtained experimentally using calorimetry, while the activity coefficient is calculated using an appropriate thermodynamic model (e.g., EOS).

For LLE calculations, which determine the miscibility regions in IBU-PLA/PLGA systems, the method of alternating tangents [24] was used in this study. When applying this method, only the composition of one of the coexisting liquid phases is sought, making it an efficient approach for LLE calculations in asymmetric mixtures such as API-polymer mixtures. The obtained binodal points have to satisfy the equilibrium condition for two coexisting phases (L1 and L2) given by the following equations:

$$\begin{aligned} x_{IBU}^{L1} \gamma_{IBU}^{L1} &= x_{IBU}^{L2} \gamma_{IBU}^{L2} \\ x_{polymer}^{L1} \gamma_{polymer}^{L1} &= x_{polymer}^{L2} \gamma_{polymer}^{L2} \end{aligned} \quad (3)$$

where γ_i^{L1} and γ_i^{L2} are IBU and polymer activity coefficients in phases L1 and L2 and x_i^{L1} and x_i^{L2} are their mole fractions, respectively.

The activity coefficients needed for both SLE and LLE calculations were obtained using the PC-SAFT EOS [25,26] in its copolymer version [27]. A brief description of the PC-SAFT EOS is provided below.

Within the PC-SAFT framework, the reduced residual Helmholtz energy (a^{res}) of a system is described as a sum of independent contributions:

$$a^{\text{res}} = a^{\text{hc}} + a^{\text{disp}} + a^{\text{assoc}} \quad (4)$$

where a^{hc} is the hard-chain contribution accounting for repulsive forces, a^{disp} is the contribution for dispersion attractive forces, and a^{assoc} is the contribution accounting for association (hydrogen bonding) interactions. In the PC-SAFT concept, each molecule i is represented as a chain of m spherical segments of the same diameter σ_i . These two parameters are used to calculate the contribution a^{hc} . The dispersion contribution a^{disp} is evaluated using the energy parameter ε_i/k (k is the Boltzmann constant) and the association contribution a^{assoc} using the energy parameter $\varepsilon_i^{\text{assoc}}/k$ and the association volume κ_i^{assoc} . Besides the five pure-component parameters mentioned above, the number of association sites N_i^{assoc} (electron donors and acceptors) must be specified based on the molecular structure of a given compound.

The PC-SAFT parameters for IBU and PLA/PLGA polymers utilized in this study are listed in Table 1. The IBU parametrization was performed in our previous study [28] using the liquid density and vapor pressure data for pure IBU in conjunction with the data on IBU solubility in selected organic solvents. IBU was modeled as a self-associating molecule with four association sites (i.e., 2 hydrogen bond (HB) donors and 2 HB acceptors). The PLGA and PLA were modeled via the copolymer version of PC-SAFT [27] in which polymers are considered as a chain of homopolymer units with their individual sets of PC-SAFT parameters. In this modification, the PC-SAFT EOS is able to account for different arrangements of monomers, composition, and molecular weight of copolymers [27,29]. The parameters for homopolymers PLLA and PDLA were obtained from Cocchi et al. [30] and those for PGA from Prudic et al. [29] (see Table 1). The monomer compositions in the copolymers studied are provided in Table 3. Both PLGA and PLA polymers are assumed to be non-associating in these parametrizations. The bond fractions between the monomer unit segments capturing the copolymer arrangements were taken from Prudic et al. [29].

Table 1. PC-SAFT EOS pure-component parameters.

Compound	$(m/M_w)_i$	σ_i (Å)	ε_i/k (K)	$\varepsilon_i^{\text{assoc}}/k$ (K)	κ_i^{assoc}	N_i^{assoc} ^a
IBU ^b	0.02636	4.0179	API	309.40	516.469	0.08946
			PLGA ^c			
PLLA ^d	0.04545	2.920	230.0	0	0	0 (0, 0)
PDLA ^d	0.03699	3.120	240.0	0	0	0 (0, 0)
PGA ^e	0.03130	2.860	233.9	0	0	0 (0, 0)

^a $N_i^{\text{assoc}}(\text{D,A})$ is the total number of hydrogen bonding (HB) sites, D is the number of HB donor sites, and A denotes the number of HB acceptor sites in a molecule. ^b Adopted from [28]. ^c PLGA and PLA properties are summarized in Tables 2 and 3. ^d Adopted from [30]. ^e Adopted from [29].

Table 2. Monomer composition (as mass fractions) in the copolymers studied.

Polymer	$w_{\text{LLA}} = w_{\text{DLA}}$	w_{GA}
PDLG 5002A/PDLG 5004A	0.277	0.446
PDLG 7502A/PDLG 7504A	0.394	0.212
PDL 02A/PDL 04A	0.500	0

Table 3. Pure-component physicochemical properties.

Compound	M_w^a (g·mol ⁻¹)	T_g^b (°C)	T_m^b (°C)	ΔH_{fus}^b (kJ·mol ⁻¹)	$\Delta C_{p,fus}^c$ (J·K ⁻¹ ·mol ⁻¹)
IBU	206.3	-45.0 ± 0.3	75.6 ± 0.3	26.4 ± 0.8	176.16440 – 0.3449480·(T/K)
PDLG 5002A	9877	39.6 ± 0.3	-	-	-
PDLG 5004A	35,900	46.7 ± 0.3	-	-	-
PDLG 7502A	12,900	38.7 ± 0.3	-	-	-
PDLG 7504A	38,800	48.8 ± 0.3	-	-	-
PDL 02A	16,400	47.8 ± 0.3	-	-	-
PDL 04A	40,200	50.4 ± 0.3	-	-	-

^a The average molecular weight (M_w) of polymers was determined in this work using gel permeation chromatography (Waters, equipped with a differential refractive index detector) based on narrow polystyrene standards. ^b This study except for T_g values for PDLG 5002A and PDLG 7502A, which were determined in the previous study [14]. Reported uncertainties correspond to the combined expanded uncertainties ($k = 2$, 0.95 level of confidence) in determining temperature and enthalpy values. ^c The difference between the isobaric molar heat capacity of a liquid and a crystal. The reported equation was derived based on experimental heat capacities published in [31].

Activity coefficients γ_i^L can be obtained from the PC-SAFT EOS using the following thermodynamic relationships [25]:

$$\ln \varphi_i^L = a^{\text{res}} + \left(\frac{\partial a^{\text{res}}}{\partial x_i} \right)_{T,\rho,x_{k \neq i}} - \sum_j \left[x_j \left(\frac{\partial a^{\text{res}}}{\partial x_j} \right)_{T,\rho,x_{k \neq j}} \right] + Z - 1 - \ln Z \quad (5)$$

$$\ln \gamma_i^L = \ln \varphi_i^L - \ln \varphi_{0,i}^L \quad (6)$$

where a^{res} is the reduced residual Helmholtz energy (Equation (4)), φ_i^L is the fugacity coefficient of IBU or polymer in the liquid mixture, $\varphi_{0,i}^L$ denotes the fugacity coefficient of the pure liquid, ρ is the molar density of the system, and Z is the compressibility factor.

Besides pure-component parameters, binary interaction parameter k_{ij} correcting the cross-dispersion energy parameter ε_{ij}/k is introduced within the PC-SAFT framework to achieve closer agreement between experimental results for mixtures and phase behavior predictions [25,26]:

$$\frac{\varepsilon_{ij}}{k} = \sqrt{\frac{\varepsilon_i}{k} \frac{\varepsilon_j}{k}} (1 - k_{ij}) \quad (7)$$

In this work, two variants of PC-SAFT calculations are presented: (i) pure predictions with $k_{ij} = 0$, i.e., the calculation based solely on pure-component parameters; and (ii) calculations with k_{ij} values optimized using experimental SLE data for the one binary system IBU–PDLG 7502A [14]. Based on the performance of pure predictions in terms of identifying phenomena, such as APS, or providing qualitative ordering of SLE data, the suitability of PC-SAFT EOS as a computational screening tool for selecting suitable polymeric carriers for further experimental investigation can be evaluated. In scenario (ii), the ability of the PC-SAFT EOS to predict complete phase diagrams based on optimized k_{ij} values using SLE data for IBU with only one polymer from the PLA/PLGA family was studied. In other words, the transferability of modeling phase behavior using PC-SAFT EOS and its ability to describe the trends in phase behavior within the PLA/PLGA family were investigated.

3. Results

3.1. Physicochemical Properties of Pure Components

The physicochemical properties of the pure materials utilized in this study are presented in Table 2. Both melting temperature and fusion enthalpy of IBU agree well with the previously published values summarized by Štejfa et al. [31]. The amorphous IBU was obtained by quenching the melt using $\beta = 20$ °C min⁻¹, and its T_g was measured during subsequent heating by $\beta = 10$ °C min⁻¹. The obtained T_g value is in alignment with

the results found in the literature, which cover the range from -48 to -45 °C [31]. The recorded T_g of the PLA/PLGA polymers are in good agreement with the general trend typical for this group of polymers described in the literature: T_g increases with increasing LA content (e.g., from 35.7 °C for PLGA 50:50 (LA:GA) to 45.3 °C for the PLA 100:0 (LA:GA) according to Pyo Park et al. [32]) and molecular weight of the polymer (e.g., from 42.2 °C for 8000 g/mol PLGA to 52.6 °C $110,000$ g/mol PLGA, in accordance with Lee et al. [33]).

3.2. IBU–PLA/PLGA Phase Diagrams

Experimental T_s and T_g values for binary systems IBU–PDL 5004A, IBU–PDL 7504A, and IBU–PDL 02A/04A are summarized in Tables S1 and S2 in the Supplementary Material (SM). T_s and T_g data for IBU–PDL 5002A and IBU–PDL 7502A were reported in our previous study [14]. The resulting phase diagrams are shown in Figure 2. The T_g line defining the kinetic stability of ASD formulations was modeled using the Kwei equation (Equation (1)) with parameters listed in Table S3 in SM. The PC-SAFT EOS, which was used to model thermodynamic phase behavior (i.e., SLE and LLE) was applied in two variants: (i) with all binary interaction parameter k_{ij} s set to zero, which represents pure prediction based solely on pure-component parameters (represented by dashed lines in Figure 2); and (ii) with k_{ij} values adjusted based on experimental SLE data for one binary system IBU–PDLG 7502A (represented by solid lines in Figure 2).

The solubility of IBU in the studied PLA and PLGA polymers obtained by pure predictions at 25 °C (typical storage temperature) is listed in Table 4. As can be seen, with k_{ij} s = 0, the solubility of IBU was predicted to be almost identical for all polymers examined (regardless of differences in polymer composition and molecular weight) and fell in the range of 21.6 to 22.7 wt.%. The PDL 02A (i.e., lower molecular weight PLA) polymer demonstrated the highest solubility potential for IBU based on pure predictions. Compared to experimental results, the predicted SLE curves considerably overestimated the IBU solubility in all studied polymers. The average absolute relative deviation (AARD) listed in Table S4 ranges from 93 to 157% . Furthermore, and most importantly, PC-SAFT EOS with k_{ij} s = 0 did not (at least qualitatively) predict the presence of the immiscibility region for any system, which was observed experimentally.

Table 4. IBU solubility w_{IBU} (wt.%) in PLA/PLGA polymers at 25 °C calculated using PC-SAFT EOS with k_{ij} s = 0 and optimized k_{ij} s.

Polymer	M_w (g·mol ⁻¹)	LA Group (mol%)	Solubility w_{IBU} (wt.%, k_{ij} s = 0)	Solubility w_{IBU} (wt.%, Optimized k_{ij} s)
Lower M_w polymers				
PDLG 5002A	9877	50	21.9	1.4
PDLG 7502A	12,900	75	22.4	1.7
PDL 02A	16,400	100	22.9	2.1
Higher M_w polymers				
PDLG 5004A	35,900	50	21.6	1.2
PDLG 7504A	38,800	75	22.2	1.6
PDL 04A	40,200	100	22.7	2.0

To achieve an improved description of experimental SLE data using PC-SAFT EOS, the temperature-independent k_{ij} s between IBU–DLA, IBU–LLA, and IBU–GA (PLGA polymers) and between IBU–LLA and IBU–DLA (PLA polymers) groups, determined based on SLE data for IBU–PDLG 7502A systems in our recent study [14], were applied. In brief, to shorten the number of fitted parameters (following the recommendation of Prudic et al. [29]), k_{ij} s between the monomeric units of the homopolymer DLA, LLA, and GA were considered to be zero, and k_{ij} s between IBU–LLA and IBU–DLA were assumed to be identical. The applied k_{ij} s are listed in Table S5.

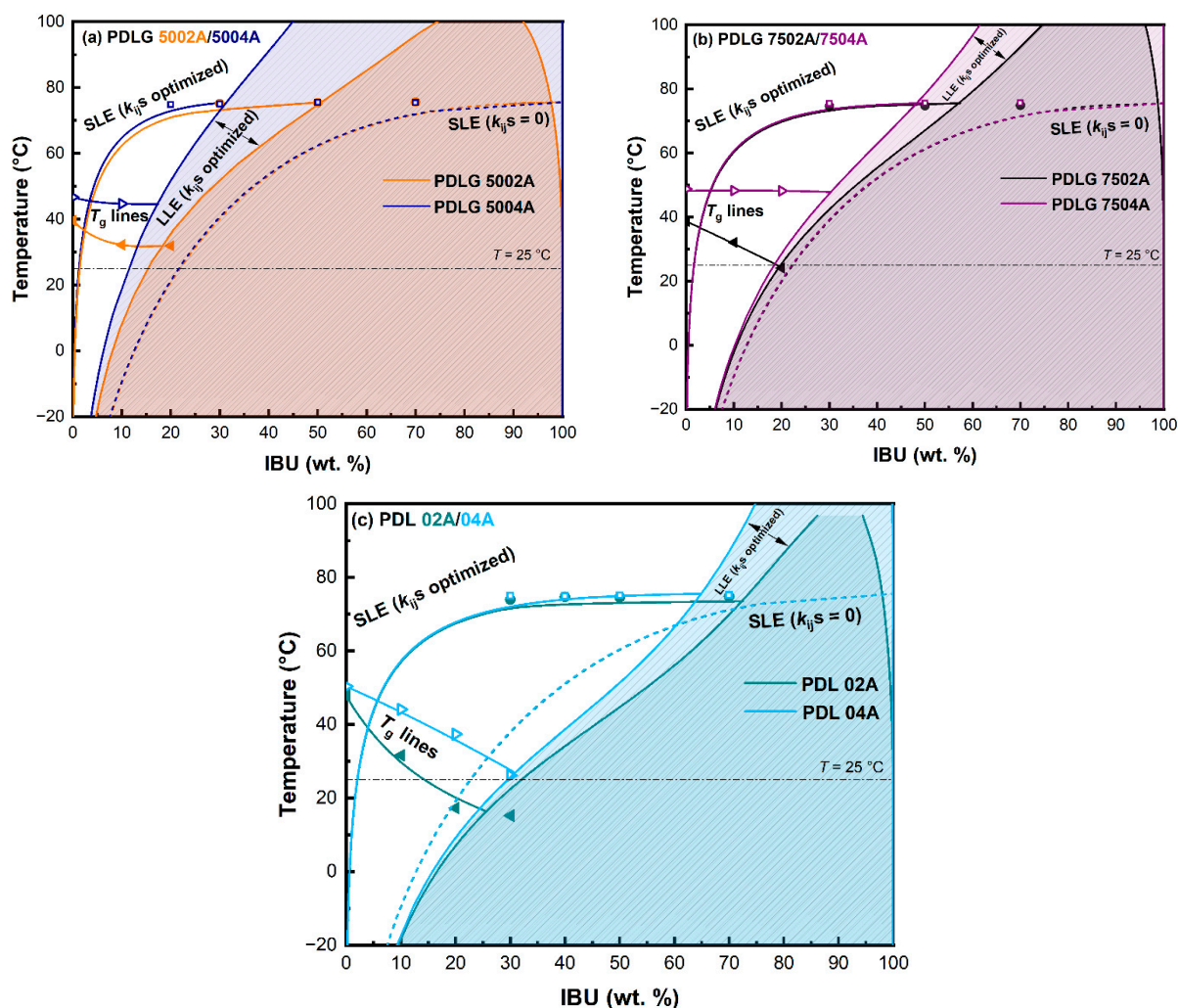


Figure 2. IBU-PLA/PLGA phase diagrams: (a) IBU-PDLG 5002A/PDLG 5004A, (b) IBU-PDLG 7502A/PDLG 7504A, and (c) IBU-PDL 02A/PDL 04A. Symbols represent experimental values and lines represent the calculated properties. T_g lines were modeled by the Kwei equation, Equation (1), and SLE and LLE using the PC-SAFT EOS. Experimental T_g and SLE values are listed in Tables S1 and S2, respectively; parameters of the Kwei equation, Equation (1), are listed in Table S3; and applied binary interaction parameters k_{ij} are listed in Table S5. Data for IBU-PDLG 5002A and IBU-PDLG 7502A were taken from our previous study [14].

Similar to the pure predictions, the impact of polymer molecular weight and composition on the evaluated solubility was relatively modest (see Table 4). The solubility of IBU at 25 °C predicted using the optimized PC-SAFT EOS was found to range from 1.2 to 2.1 wt.%. As for pure predictions, the solubility of IBU in PDL 02A was predicted to be the highest among the studied polymers. The corresponding AARD values lying in the range from 23.3% (PDL 02A) to 33.4% (PDLG 5004A) are shown in Table S4. Such high AARDs can be explained by the incapacity of PC-SAFT together with k_{ij} s (temperature-independent) to accommodate a weak dependence of experimental IBU solubility on the temperature in PLA and PLGA polymers (squares and circles in Figure 2). Nonetheless, the PC-SAFT model with the adjusted k_{ij} s was able to qualitatively predict the presence of liquid–liquid phase splitting events in the IBU-PLA and IBU-PLGA systems, which is in agreement with experimental observations (for details, see Section 3.3).

In accordance with Equation (7), the positive k_{ij} denotes the reduction of API–polymer interactions, which, in turn, leads to a decrease in solubility and miscibility. It can be clearly visible for IBU-PLGA and IBU-PLA systems, where relatively high positive values of

k_{ij} (Table S5) resulted in very limited solubility values (at 25 °C) of the studied systems (see Table 4). Moreover, it can be observed from Figure 2 that, although the polymer composition (i.e., the content of LLA/DLA or GA units) or molecular weight demonstrated only a slight impact on calculated IBU solubility (SLE), the effect on LLE binodal curve was more pronounced, which indicates a higher sensitivity of APS calculations on the model parameters (for details, see Section 3.3). These observations are consistent with the results obtained in the previous study [14] and those by Sadowski and co-authors [29,34].

The corresponding T_g lines were constructed to determine the regions where the IBU–PLGA and IBU–PLA ASD formulations can be stabilized kinetically owing to considerably lower molecular motion at conditions under the T_g line. As can be seen from the phase diagrams depicted in Figure 2, at a typical storage temperature of 25 °C, ASD formulations with drug loadings higher than a couple of weight percentages are estimated to be thermodynamically unstable as their temperature-composition coordinates are located on the right from the SLE curve. Therefore, the physical stability of ASD formulations (with $w_{IBU} > 2$ wt.% at 25 °C) will be governed by kinetic aspects, i.e., by the difference between the storage temperature and T_g line. Based on T_g lines depicted in the phase diagrams (Figure 2), a higher kinetic stabilization of ASD formulations consisting of higher molecular weight polymers can be deduced, which represents an advantage of using higher molecular weight PLA/PLGA polymers in ASD-based drug delivery systems.

3.3. Miscibility of IBU with PLA/PLGA Polymers

For all binary systems studied, APS (LLE) was observed during the solubility measurements using the MPD method. To outline approximate phase boundaries for APS, i.e., to identify temperature-composition regions at which APS occurs, a series of complementary melt quenching calorimetric experiments was conducted. The calorimetric mapping consisted of the determination of T_g for binary IBU–PLA/PLGA mixtures, which were annealed at temperatures above IBU melting temperature for fixed composition and subsequently quenched to –90 °C. The maximum annealing temperature was set to 150 °C to avoid the thermal decomposition of IBU. A single T_g value located between T_g of pure IBU and pure PLA/PLGA polymer was considered to indicate a single homogenous amorphous mixture, while two T_g values observed close to T_g of pure IBU and that of pure polymer were considered to indicate of creation of a two-phase system comprising polymer-rich and IBU-rich phases. The mapping outcomes together with the LLE region predicted using PC-SAFT EOS (optimized k_{ij} s) are depicted schematically in Figure 3. The T_g values determined during the mapping experiments are summarized in Table S2.

Based on the approximate areas of immiscibility regions obtained during the mapping experiments (Figure 3), the following ranking of experimental miscibility of the polymers studied with IBU can be deduced: PDL 04A > PDL 02A > PDLG 7504A > PDLG 7502A > PDLG 5002A > PDLG 5004A. Considering these results, the impact of the polymer composition is clearly visible: the higher LA content, the smaller LLE region (i.e., the higher mutual miscibility of IBU and polymer). At the same time, the impact of the molecular weight of the polymer is not as obvious. In the case of IBU–PDL 04 and IBU–PDLG 7504A systems, the determined LLE region was noticeably smaller compared to the systems of IBU with lower molecular weight analogs (i.e., PDL 02A and PDLG 7502). However, the situation with PDLG 5002A and PDLG 5004A (i.e., LA to GA ratio 50:50) was the opposite.

The results of LLE modeling using PC-SAFT with optimized k_{ij} s are presented and compared with experimental results in Figure 3 (modeling with k_{ij} s = 0 did not indicate LLE). The equilibrium concentrations predicted using the PC-SAFT for the polymer-rich phase at 25 °C are summarized in Table 5. Based on these results, the following miscibility trend was derived: w_{IBU} (PDL 02A) > w_{IBU} (PDL 04A) > w_{IBU} (PDLG 7502A) > w_{IBU} (PDLG 7504A) > w_{IBU} (PDLG 5002A) > w_{IBU} (PDLG 5004A).

Table 5. Miscibility limit w_{IBU} (wt.%, polymer-rich phase) at 25 °C calculated using the PC-SAFT with $k_{ij}s = 0$ and optimized $k_{ij}s$.

Polymer	M_w (g·mol ⁻¹)	LA Group (mol%)	APS w_{IBU} (wt.%, $k_{ij}s = 0$)	APS w_{IBU} (wt.%, Optimized $k_{ij}s$)
Lower M_w polymers				
PDLG 5002A	9877	50	-	15.4
PDLG 7502A	12,900	75	-	19.8
PDL 02A	16,400	100	-	31.9
Higher M_w polymers				
PDLG 5004A	35,900	50	-	11.5
PDLG 7504A	38,800	75	-	18.4
PDL 04A	40,200	100	-	29.6

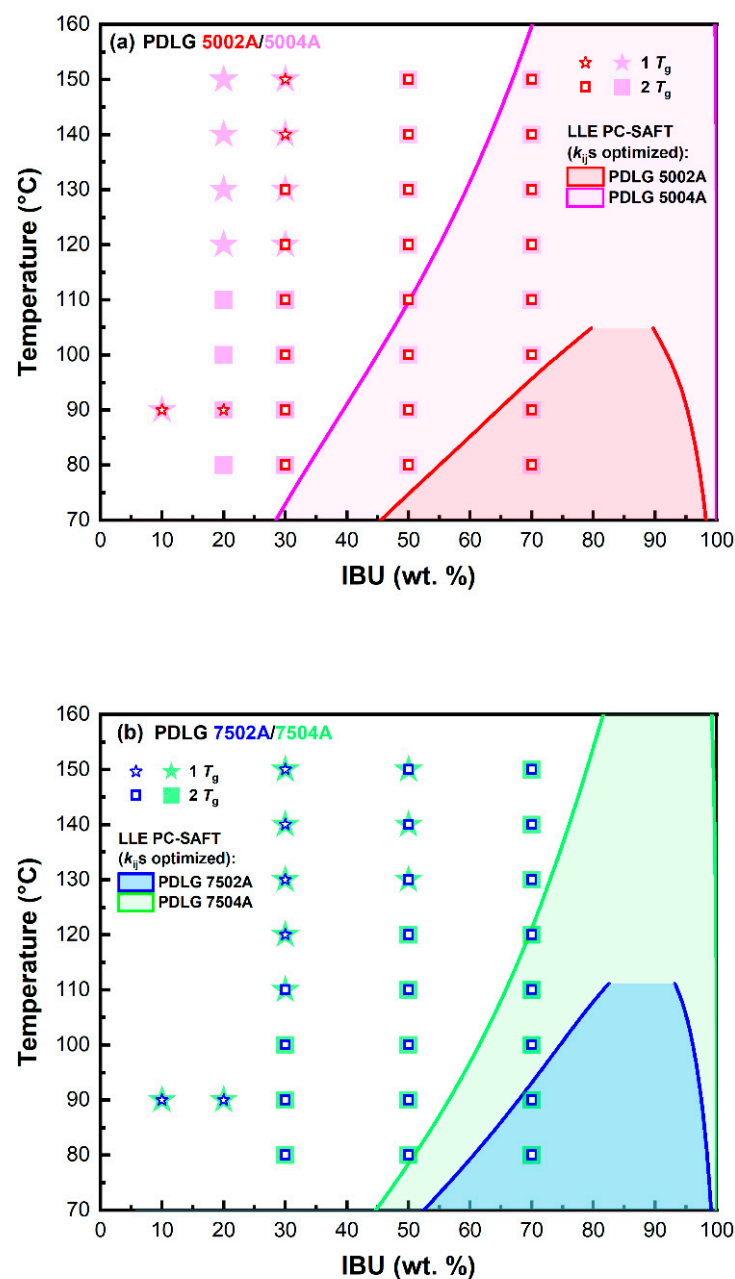


Figure 3. Cont.

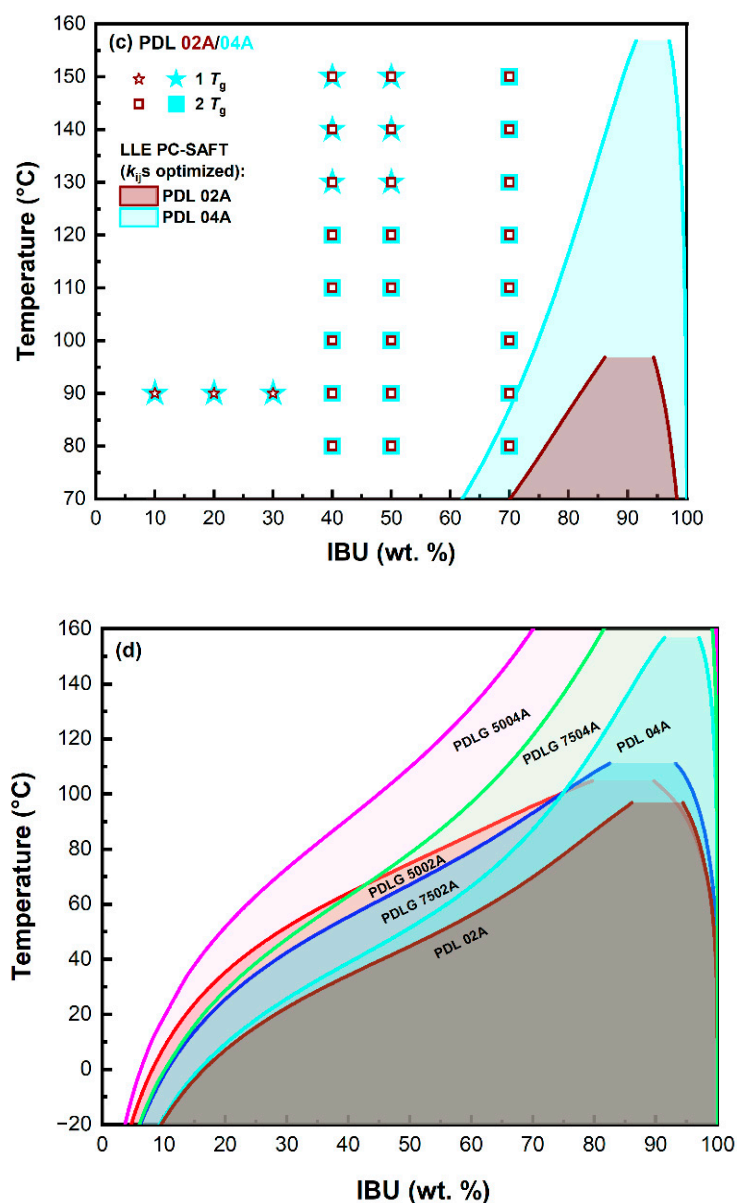


Figure 3. Comparison of LLE areas determined using DSC measurements with those predicted using the PC-SAFT EOS: (a) PDLG 5002A/5004A, (b) PDLG 7502A/7504A, and (c) PDL 02A/04A. (d) Comparison of LLE regions modeled by PC-SAFT.

For both lower and higher molecular weight polymers, the miscibility between the IBU and polymer increases with increasing LA content, reflecting a higher number of favorable hydrophobic interactions between IBU and LA. These findings qualitatively agree with the experimental results obtained in this work as well as with the results obtained by Luebbert et al. [34] for low molecular weight PLGA and PLA polymers. Regarding the impact of molecular weight at fixed copolymer composition, the experimental mapping of APS suggests that the mutual miscibility of IBU with the polymer increases with increasing polymer molecular weight for polymers with LA content of 75 and 100 mol.%. LLE calculations by PC-SAFT with optimized $k_{ij}s$ do not capture this trend.

The prediction of the conditions under which the components are miscible is a key parameter in designing homogeneous drug formulations and predicting their long-term physical stability. At the same time, LLE calculations are extremely challenging, especially when considering asymmetrical mixtures such as API–polymer mixtures. As mentioned above, PC-SAFT EOS without optimization using SLE experimental data was unable to

signal a possible immiscibility region for the binary systems studied, which is contrary to experimental evidence. This can be considered as a significant limitation if PC-SAFT EOS is to be considered as an *in silico* screening tool for the selection of suitable polymeric excipients for a given API. In order to detect a possible liquid–liquid split or APS using PC-SAFT EOS, the experimental SLE data should be provided and used for the optimization of binary interaction parameters k_{ij} (we note that, in this work, k_{ij} values were derived based on SLE data for only one binary system, IBU–PDLG 7502A). With the optimized k_{ij} values, PC-SAFT EOS correctly predicted the presence of immiscibility region for all the binary systems studied, although compared to experimental results, the size of heterogenous regions was systematically underestimated.

4. Conclusions

Herein, the thermodynamic phase behavior of IBU with PLA/PLGA polymers of various molecular weights and copolymer compositions was investigated experimentally using calorimetry and computationally using PC-SAFT EOS. Kinetic stability was estimated on the basis of the T_g line modeled using the Kwei equation. The constructed phase diagrams indicate a very low solubility of IBU in PLA/PLGA polymers at a typical storage temperature of 25 °C, limited miscibility of IBU with PLA/PLGA polymers, and increasing kinetic stability with increasing molecular weight of PLA/PLGA polymers. While the effect of copolymer composition or molecular weight on the solubility of IBU was minimal, it had a more pronounced impact on the size of the miscibility region. The PC-SAFT predictions using solely pure-component parameters for IBU and PLA/PLGA polymers (i.e., pure predictions without any experimental input for a given binary system) significantly overestimated IBU solubility and provided no evidence of possible liquid–liquid split or amorphous phase separation. After optimizing binary interaction parameters k_{ij} using SLE experimental data (based on SLE data for one of the six binary systems studied), the PC-SAFT EOS correctly detected a possible formation of a heterogeneous immiscibility region for all the binary systems studied. Using optimized k_{ij} values, the PC-SAFT EOS system was able to capture miscibility trends as a function of copolymer composition, while the effect of molecular weight was only partially captured, and the miscibility region was systematically underestimated compared to experimental results.

Supplementary Materials: The following supporting information can be downloaded at: <https://www.mdpi.com/article/10.3390/pharmaceutics15020645/s1>, Table S1: T_g values obtained for IBU–PLGA and IBU–PLA systems; Table S2: (a) T_g values obtained for IBU–PDLG 5004A system annealed at 80–150 °C. (b) T_g values obtained for IBU–PDLG 7504A system annealed at 80–150 °C. (c) T_g values obtained for IBU–PDL 02A system annealed at 80–150 °C. (d) T_g values obtained for IBU–PDL 04A system annealed at 80–150 °C; Table S3: Parameters k and q of the Kwei equation ((Equation (1) in the main article) for IBU–PLGA and IBU–PLA systems; Table S4: AARD (w_{API}) values between experimental SLE data and data calculated using PC-SAFT EOS for all IBU–PLGA and IBU–PLA systems; Table S5: PC-SAFT EOS binary interaction parameters, k_{ij} , between the IBU and the different monomer units of PLA/PLGA polymers.

Author Contributions: A.I.: Investigation, Formal analysis, Visualization, Writing—original draft. M.K.: Software, Writing—review and editing. F.H.: Conceptualization, Methodology, Formal analysis, Supervision, Writing—review and editing. M.F.: Conceptualization, Methodology, Supervision, Formal analysis, Writing—original draft, Writing—review and editing. All authors have read and agreed to the published version of the manuscript.

Funding: This research was funded by Czech Science Foundation (GAČR No. 22-07164S) and by the grants of specific university research (A2_FCHI_2022_002 and A1_FCHI_2022_002).

Institutional Review Board Statement: Not applicable.

Informed Consent Statement: Not applicable.

Data Availability Statement: All data relevant to the publication are included.

Acknowledgments: The authors would like to acknowledge the Zentiva Group (Prague, Czech Republic) and Corbion (Gorinchem, Netherlands) for the chemicals donated to conduct this research.

Conflicts of Interest: The authors declare no conflict of interest.

References

1. Savjani, K.T.; Gajjar, A.K.; Savjani, J.K. Drug Solubility: Importance and Enhancement Techniques. *ISRN Pharm.* **2012**, *2012*, 195727. [CrossRef] [PubMed]
2. He, Y.; Ho, C. Amorphous Solid Dispersions: Utilization and Challenges in Drug Discovery and Development. *J. Pharm. Sci.* **2015**, *104*, 3237–3258. [CrossRef] [PubMed]
3. Khan, K.U.; Minhas, M.U.; Badshah, S.F.; Suhail, M.; Ahmad, A.; Ijaz, S. Overview of nanoparticulate strategies for solubility enhancement of poorly soluble drugs. *Life Sci.* **2022**, *291*, 120301. [CrossRef] [PubMed]
4. Makadia, H.K.; Siegel, S.J. Poly Lactic-co-Glycolic Acid (PLGA) as Biodegradable Controlled Drug Delivery Carrier. *Polymers* **2011**, *3*, 1377–1397. [CrossRef] [PubMed]
5. Wang, Y.; Qu, W.; Choi, S.H. FDA's Regulatory Science Program for Generic PLA/PLGA-Based Drug Products. *Am. Pharm. Rev.* **2016**, *20*. Available online: <https://www.americanpharmaceuticalreview.com/Featured-Articles/188841-FDA-s-Regulatory-Science-Program-for-Generic-PLA-PLGA-Based-Drug-Products/> (accessed on 19 December 2022).
6. Erbetta, C. Synthesis and Characterization of Poly(D,L-Lactide-co-Glycolide) Copolymer. *J. Biomater. Nanobiotechnol.* **2012**, *3*, 208–225. [CrossRef]
7. Nieto, K.; Mallery, S.; Schwendeman, S. Microencapsulation of Amorphous Solid Dispersions of Fenretinide Enhances Drug Solubility and Release from PLGA in vitro and in vivo. *Int. J. Pharm.* **2020**, *586*, 119475. [CrossRef]
8. Bohr, A.; Kristensen, J.; Stride, E.; Dyas, M.; Edirisinghe, M. Preparation of microspheres containing low solubility drug compound by electrohydrodynamic spraying. *Int. J. Pharm.* **2011**, *412*, 59–67. [CrossRef]
9. Bala, I.; Hariharan, S.; Kumar, M.N.V.R. PLGA Nanoparticles in Drug Delivery: The State of the Art. *Crit. Rev. Ther. Drug Carr. Syst.* **2004**, *21*, 387–422. [CrossRef] [PubMed]
10. Panyam, J.; Williams, D.; Dash, A.; Leslie-Pelecky, D.; Labhasetwar, V. Solid-state solubility influences encapsulation and release of hydrophobic drugs from PLGA/PLA nanoparticles. *J. Pharm. Sci.* **2004**, *93*, 1804–1814. [CrossRef] [PubMed]
11. Blasi, P. Poly(lactic acid)/poly(lactic-co-glycolic acid)-based microparticles: An overview. *J. Pharm. Investig.* **2019**, *49*, 337–346. [CrossRef]
12. Zumaya, A.L.V.; Ulbrich, P.; Vilčáková, J.; Dendisová, M.; Fulem, M.; Šoóš, M.; Hassouna, F. Comparison between two multicomponent drug delivery systems based on PEGylated-poly (l-lactide-co-glycolide) and superparamagnetic nanoparticles: Nanoparticulate versus nanocluster systems. *J. Drug Deliv. Sci. Technol.* **2021**, *64*, 102643. [CrossRef]
13. Zumaya, A.L.V.; Martynek, D.; Bautkinová, T.; Šoóš, M.; Ulbrich, P.; Raquez, J.-M.; Dendisová, M.; Merna, J.; Vilčáková, J.; Kopecký, D.; et al. Self-assembly of poly(L-lactide-co-glycolide) and magnetic nanoparticles into nanoclusters for controlled drug delivery. *Eur. Polym. J.* **2020**, *133*, 109795. [CrossRef]
14. Iemtsev, A.; Hassouna, F.; Klajmon, M.; Mathers, A.; Fulem, M. Compatibility of selected active pharmaceutical ingredients with poly(D, L-lactide-co-glycolide): Computational and experimental study. *Eur. J. Pharm. Biopharm.* **2022**, *179*, 232–245. [CrossRef]
15. Mahieu, A.; Willart, J.-F.; Dudognon, E.; Danède, F.; Descamps, M. A New Protocol To Determine the Solubility of Drugs into Polymer Matrixes. *Mol. Pharm.* **2013**, *10*, 560–566. [CrossRef]
16. Marsac, P.J.; Shamblin, S.L.; Taylor, L.S. Theoretical and Practical Approaches for Prediction of Drug–Polymer Miscibility and Solubility. *Pharm. Res.* **2006**, *23*, 2417. [CrossRef]
17. Sun, Y.; Tao, J.; Zhang, G.G.Z.; Yu, L. Solubilities of Crystalline Drugs in Polymers: An Improved Analytical Method and Comparison of Solubilities of Indomethacin and Nifedipine in PVP, PVP/VA, and PVAc. *J. Pharm. Sci.* **2010**, *99*, 4023–4031. [CrossRef] [PubMed]
18. Gill, P.; Moghadam, T.T.; Ranjbar, B. Differential scanning calorimetry techniques: Applications in biology and nanoscience. *J. Biomol. Tech.* **2010**, *21*, 167–193.
19. Mathers, A.; Hassouna, F.; Klajmon, M.; Fulem, M. Comparative Study of DSC-Based Protocols for API–Polymer Solubility Determination. *Mol. Pharm.* **2021**, *18*, 1742–1757. [CrossRef] [PubMed]
20. Höhne, G.W.H.; Hemminger, W.; Flammersheim, H.-J. *Differential Scanning Calorimetry*; Springer: Berlin/Heidelberg, Germany, 2003; Volume 2.
21. Kwei, T.K. The effect of hydrogen bonding on the glass transition temperatures of polymer mixtures. *J. Polym. Sci. Polym. Lett. Ed.* **1984**, *22*, 307–313. [CrossRef]
22. Simha, R.; Boyer, R.F. On a General Relation Involving the Glass Temperature and Coefficients of Expansion of Polymers. *J. Chem. Phys.* **1962**, *37*, 1003–1007. [CrossRef]
23. Iemtsev, A.; Hassouna, F.; Mathers, A.; Klajmon, M.; Dendisová, M.; Malinová, L.; Školáková, T.; Fulem, M. Physical stability of hydroxypropyl methylcellulose-based amorphous solid dispersions: Experimental and computational study. *Int. J. Pharm.* **2020**, *589*, 119845. [CrossRef]
24. Von Solms, N.; Kouskoumvekaki, I.A.; Lindvig, T.; Michelsen, M.L.; Kontogeorgis, G.M. A novel approach to liquid-liquid equilibrium in polymer systems with application to simplified PC-SAFT. *Fluid Phase Equilib.* **2004**, *222*, 87–93. [CrossRef]

25. Gross, J.; Sadowski, G. Perturbed-Chain SAFT: An Equation of State Based on a Perturbation Theory for Chain Molecules. *Ind. Eng. Chem. Res.* **2001**, *40*, 1244–1260. [[CrossRef](#)]
26. Gross, J.; Sadowski, G. Application of the Perturbed-Chain SAFT Equation of State to Associating Systems. *Ind. Eng. Chem. Res.* **2002**, *41*, 5510–5515. [[CrossRef](#)]
27. Gross, J.; Spuhl, O.; Tumakaka, F.; Sadowski, G. Modeling copolymer systems using the perturbed-chain SAFT equation of state. *Ind. Eng. Chem. Res.* **2003**, *42*, 1266–1274. [[CrossRef](#)]
28. Klajmon, M. Investigating Various Parametrization Strategies for Pharmaceuticals within the PC-SAFT Equation of State. *J. Chem. Eng. Data.* **2020**, *65*, 5753–5767. [[CrossRef](#)]
29. Prudic, A.; Lesniak, A.K.; Ji, Y.H.; Sadowski, G. Thermodynamic phase behaviour of indomethacin/PLGA formulations. *Eur. J. Pharm. Biopharm.* **2015**, *93*, 88–94. [[CrossRef](#)]
30. Cocchi, G.; Angelis, M.G.D.; Sadowski, G.; Doghieri, F. Modelling polylactide/water/dioxane systems for TIPS scaffold fabrication. *Fluid Phase Equilib.* **2014**, *374*, 1–8. [[CrossRef](#)]
31. Štejfa, V.; Pokorný, V.; Mathers, A.; Růžička, K.; Fulem, M. Heat capacities of selected active pharmaceutical ingredients. *J. Chem. Thermodyn.* **2021**, *163*, 106585. [[CrossRef](#)]
32. In Pyo Park, P.; Jonnalagadda, S. Predictors of glass transition in the biodegradable poly-lactide and poly-lactide-co-glycolide polymers. *J. Appl. Polym. Sci.* **2006**, *100*, 1983–1987. [[CrossRef](#)]
33. Lee, J.; Chae, G.; Khang, G.; Kim, M.; Cho, S.; Lee, H. The effect of gamma irradiation on PLGA and release behavior of BCNU from PLGA wafer. *Macromol. Res.* **2003**, *11*, 352–356. [[CrossRef](#)]
34. Luebbert, C.; Huxoll, F.; Sadowski, G. Amorphous-Amorphous Phase Separation in API/Polymer Formulations. *Molecules* **2017**, *22*, 296. [[CrossRef](#)] [[PubMed](#)]

Disclaimer/Publisher’s Note: The statements, opinions and data contained in all publications are solely those of the individual author(s) and contributor(s) and not of MDPI and/or the editor(s). MDPI and/or the editor(s) disclaim responsibility for any injury to people or property resulting from any ideas, methods, instructions or products referred to in the content.